Basic Concepts of MR Imaging, Diffusion MR Imaging, and Diffusion Tensor Imaging

Eduardo H.M.S.G. de Figueiredo, BSc[a,*],
Arthur F.N.G. Borgonovi, BSc[b,c], Thomas M. Doring, MSc[d,e]

KEYWORDS

- Magnetic resonance imaging • Diffusion-weighted imaging
- Diffusion tensor imaging

BASIC PHYSICS OF MAGNETIC RESONANCE

Magnetic resonance (MR) imaging stems from the application of nuclear magnetic resonance (NMR) to radiological imaging. The adjective "magnetic" refers to the use of magnetic fields and "resonance" refers to the need of matching the frequency of an oscillating electromagnetic field to the "precessional" frequency of the spin of some nuclei in a tissue molecule.[1]

Interest in medical diagnostic possibilities of NMR began in 1971, with the study by Damadian[2] of the differences in relaxation times T1 and T2, among different tissues, and between normal and cancerous tissues.[3] In 1973, the imaging area for MR started with pioneering articles published by Lauterbur[4] and Mansfield and Grannell,[5] when the idea of spatial varying magnetic fields to give the localization information was first introduced.

The phenomenon of magnetic resonance is based on the interaction between external magnetic fields and nuclei, which have a nonzero magnetic moment. According to classical theory of electromagnetism, individual nuclear moments called spins in a static magnetic field B_0 precess with Larmor frequency w_0 about B_0. A bulk of spins forms the net magnetization vector pointing along B_0. When radiofrequency (RF) is applied in this system at Larmor frequency, the spins absorb the radiofrequency energy and the net magnetization vector flips by a certain angle in relation to B_0. The net magnetization vector can be decomposed into 2 components, a longitudinal component parallel to B_0 and a transversal component perpendicular to B_0. As the transversal component precesses around a receiver coil, it induces a current in that coil, in accordance with Faraday's law of induction. This current becomes the MR signal.[6]

After stopping sending RF to the spins system, the MR signal decays mainly via 2 processes: loss of phase between spins and energy release to the environment. The loss of phase between spins can occur due to interaction spin-spin, and this process is described as T2 relaxation, or it can occur due to B_0 inhomogeneities, described as T2* relaxation. In both ways, the transverse component of net magnetization vector decreases and even though there is energy in the system, the

[a] GE Healthcare, Avenida das Nações Unidas, 8501, 3 andar, 05425-070, São Paulo, São Paulo, Brazil
[b] Hospital das Clínicas, Avenida Dr. Enéas de Carvalho Aguiar, 255, 3 andar, 05403-900, São Paulo, São Paulo, Brazil
[c] Hospital do Coração, Avenida Dr. Enéas de Carvalho Aguiar, 255, 3 andar, 05403-900, São Paulo, São Paulo, Brazil
[d] Federal University of Rio de Janeiro, Avenida das Américas, 4666, grupo302A, Barra da Tijuca, Rio de Janeiro, Rio de Janeiro, Brazil
[e] Clínica de Diagnóstico por Imagem, Avenida das Américas, 4666, grupo302A, Barra da Tijuca, Rio de Janeiro, Rio de Janeiro, Brazil
* Corresponding author.
E-mail address: eduardo.figueiredo@ge.com

Magn Reson Imaging Clin N Am 19 (2011) 1–22
doi:10.1016/j.mric.2010.10.005
1064-9689/11/$ – see front matter

MR signal decays. The interaction between spins and the environment they insert, called spin-lattice interaction and described as T1 relaxation, causes the spins that form the net magnetization vector to release their energy, and its longitudinal component grows back along the B_0 direction.

The tissue relaxation characteristics are expressed in image contrast and are controlled by the pulse sequence chosen. The "pulse sequence" is a sequence of RF pulses, magnetic field gradient pulses, signal sampling, and time periods between them. RF pulses are basically responsible for excitation of spins and their manipulation to obtain a signal echo. Magnetic field gradients are responsible for selecting the slice to be imaged, spatially encoding the signal induced in receiver coils, using frequency and phase as location information and in some pulse sequences, gradients also control the image contrast. Spin echo and gradient echo are examples of pulse sequences that control image contrast, by applying RF pulses or gradient pulses, respectively.

Although tissue relaxation characteristics are the main source of contrast information, MR images can represent other aspects of the biologic architecture. Random thermal motion of spins in a gradient field causes a phase shift of their transverse magnetization with respect to static spins, and can be used as a source of contrast using proper pulse sequence. To better understand this mechanism of image acquisition, a brief overview of MR physics is presented in this article.

Magnetic Resonance Concepts

MR imaging works because, in the presence of an external magnetic field, one can measure the interaction between protons in human body and the external magnetic field itself. Protons interact with the external magnetic field, due to an intrinsic magnetic characteristic called spin. The classical view of spin is the effect of one charged particle—a proton, for example—spinning around itself, which creates a magnetic moment pointing perpendicularly toward a spinning axis (**Fig. 1**). In the presence of an external magnetic field, this proton behaves similarly to a magnetic bar, tending to align to the field and precesses around it.

When we are dealing with individual protons, we need to look at them through "quantum mechanical glasses," and "not-so-intuitive" thoughts are permitted under this treatment. A not-intuitive behavior is that this proton can align in either a parallel or an antiparallel orientation to the external magnetic field. There is a difference of energy between a parallel and an antiparallel state, and if this exact amount of energy is matched by an incident radiation and is delivered to the proton, it absorbs this energy and changes from one state to another. This phenomenon is called magnetic resonance. The difference of energy states depends on the magnitude of the external magnetic field B_0 where this proton is inserted, and is expressed in terms of the Larmor equation (1) as:

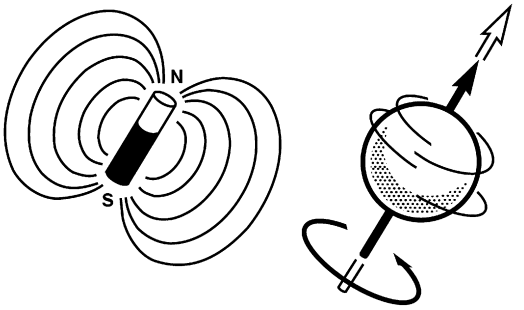

Fig. 1. In the classical view, a charged particle with spin can be compared as a magnetic dipole such as a bar magnet. (*Courtesy of* GE Healthcare, São Paulo, Brazil.)

$$w_0 = yB_0 \quad \textbf{(1)}$$

In equation (1), w_0 is the frequency needed from the incident electromagnetic field to match the energy difference between states of nuclei, with the gyromagnetic constant y in the presence of an external magnetic field of amplitude B_0. The gyromagnetic constant y is an important nucleus characteristic. Human body abundance and proper gyromagnetic constant make hydrogen nuclei (H^+) the best choice for magnetic resonance imaging.

But in MR imaging, we are not dealing with a single spin and instead of a quantum mechanics view, a classical treatment can be used to understand MR imaging physics. In a classical mechanics view, spins in the presence of an external magnetic field B_0 start to precess around B_0, with an angular frequency w_0 (**Fig. 2**). The precessional frequency is given by the same relationship expressed in quantum mechanics treatment, the Larmor equation.

The sum of many spins rotating around B_0 forms the magnetization vector M that points in the same direction as B_0. When RF wave in resonance frequency w_0 irradiates the bulk of spins, the quantum effect of states transition is analogous to flip the vector M by a certain angle in relation to B_0. If RF in resonance frequency is applied by a certain time that flips the vector M 90°, this RF pulse is said to be a "90° RF pulse." The same nomenclature applies to a "180° RF pulse."

Consider the following experiment: a bulk of spins in the presence of external magnetic field B_0. At this time, the equilibrium time, vector M,

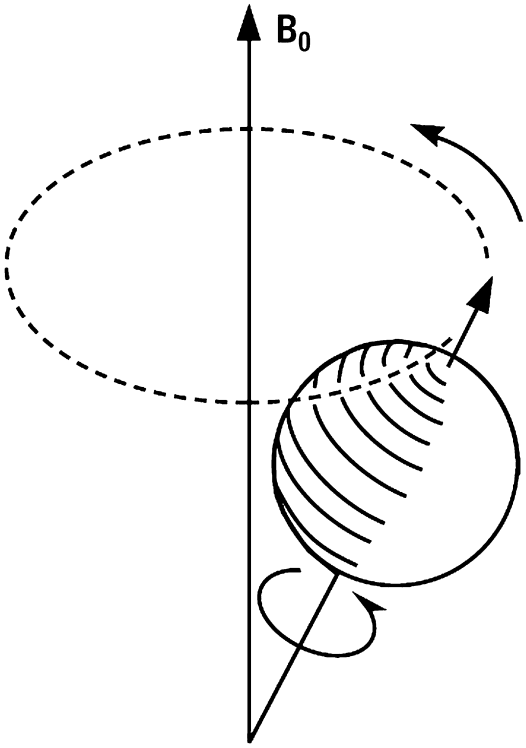

Fig. 2. Precession of spin axis around B_0. (*Courtesy of* GE Healthcare, São Paulo, Brazil.)

possesses only the longitudinal component M_z. A 90° RF pulse is applied. After turning RF off, vector M has only the transversal component M_{xy} and under the influence of B_0 starts to precess around it. At this time, vector M induces current in the receiver coil, according to Faraday's law of induction, and generates the MR signal (**Fig. 3**). When it passes through the receiver coil a maximum signal is obtained, and when it is the farthest from the coil a minimal signal is obtained. Plotting signal versus time, a sinusoidal function is to be expected.

But instead of a simple sinusoidal function, a sinusoidal function with amplitude decrease over time is obtained (**Fig. 4**). The signal represented in **Fig. 4** is called FID (free induction decay), which decays due to a process known as relaxation.

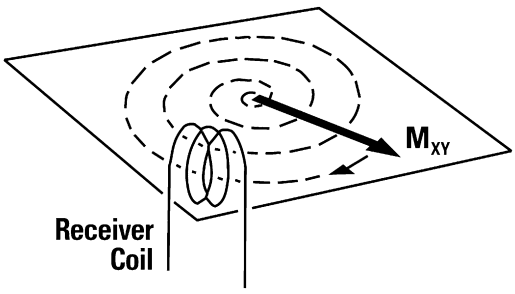

Fig. 3. In the transversal plane, rotating magnetization vector M induces current in receiver coil according to Faraday's law of induction. (*Courtesy of* GE Healthcare, São Paulo, Brazil.)

Relaxation Effects

Signal relaxation is a result of loss of phase between spins and energy release to the environment where spins are inserted. Immediately after a 90° RF pulse, all spins that form the M_{xy} vector are pointing in the same direction, and they are said to be "in phase." Turning RF off, they are set free to precess around B_0, and they precess with an angular frequency according to the Larmor equation. The first problem is that not all spins feel the same static field, due to B_0 inhomogeneities, and as they feel differently, they precess with different frequencies. This difference causes a loss of phase between them and after some time carrying out vector addition, it can be understood why the signal vanishes (**Fig. 5**). This process is called T2* decay or T2* relaxation, and effects of this nature can be restored once it is not a random effect but a scanner characteristic.

The same loss of phase described here can happen even though scanner B_0 homogeneity is perfect. Spins that form vector M_{xy} can interact with each other, feeling the tiny magnetic field of neighboring spins, in addition to B_0, and each spin starts to precess with a different frequency, resulting in the same loss of phase caused by B_0 inhomogeneities. The central difference is that this loss of phase cannot be recovered once thermal motion of spins is random. This process is called T2 relaxation or T2 decay. T2* and T2 decay express exponential behavior (see **Fig. 4**) and are modeled in terms of transversal components of vector M.

Another source of signal decay is spins giving up energy, which are absorbed by an RF pulse to the

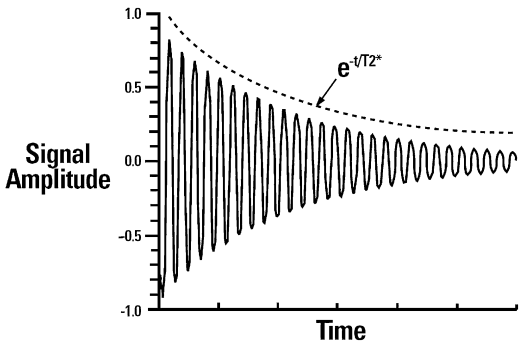

Fig. 4. MR signal amplitude (proportional to M vector magnitude) as function of time. The exponential damped sine function is called FID and is characterized by relaxation effect. (*Courtesy of* GE Healthcare, São Paulo, Brazil.)

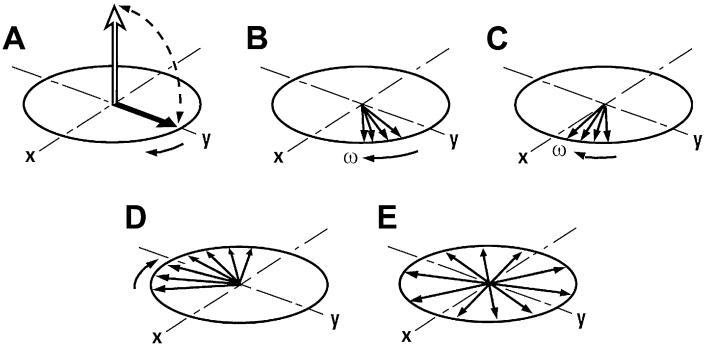

Fig. 5. Signal loss due to dephasing between spins, caused by T2* and T2 relaxation. (*Courtesy of* GE Healthcare, São Paulo, Brazil.)

environment. In terms of magnetization vectors, vector M_{xy} decreases and M_z increases over time, until all energy has been released and the vector M has only a longitudinal component (**Fig. 6**), returning to equilibrium. The energy exchange is governed by the interaction between spins and the lattice, and it is called T1 decay or T1 relaxation.

T1, T2, and T2* are tissue properties, and are measured in seconds (T2* carries B_0 inhomogeneities information, caused by the tissue and the scanner). T1 is the time needed for M_z to achieve approximately 63% of its initial value, after a 90° RF pulse. T2 and T2* are the times taken for M_{xy} to achieve approximately 37% of its initial value, after a 90° RF pulse, T2* being measured taking into account inhomogeneity effects and T2 being measured taking into account only spin-spin interactions. Image contrast contains all relaxation effects, but usually they are weighted in one effect, meaning that differences in the gray scale mostly represent differences in tissue relaxation properties. Image weighting is controlled by pulse sequences.

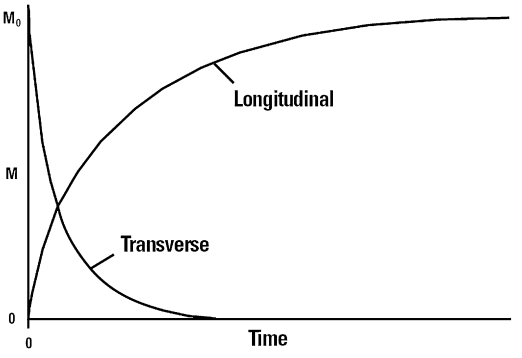

Fig. 6. The decay of transverse magnetization occurs by means of T2 and T2* effects, while recovery of longitudinal magnetization reflects energy transference to the environment. (*Courtesy of* GE Healthcare, São Paulo, Brazil.)

Pulse Sequences

In the circumstance whereby the external magnetic field is not particularly uniform, dephasing between spins caused by field inhomogeneities are the main source of signal loss. Fortunately, this effect can be reversed by a well-known RF pulse sequence called the "spin echo method."

The spin echo sequence is based on the application of 2 RF pulses: a 90° RF pulse (or excitation pulse) followed by a 180° RF pulse (or refocusing pulse). The 90° RF pulse tips all spins that form the vector M into a transversal plane and immediately after they reach the plane, they are in phase and M_{xy} has its maximum amplitude. After turning the RF pulse off, spins start to precess and lose phase by T2* relaxation effects. The 180° RF pulse is applied after a time t, defined as t = TE/2 (t is set equal to 0 at the time the first 90° RF pulse is applied), rotating the spins by 180° in relation to the position they were in. At the end of refocusing the pulse application, the spins localization remains in the transversal plane, but "faster" spins with higher precessional frequency are put behind "slower" spins with lower precessional frequency. The accumulated phase between spins caused by field inhomogeneities through the time from t = 0 seconds to t = TE/2 seconds is compensated after a 180° RF pulse at the time t = TE seconds (called echo time), TE/2 seconds after refocusing pulse. The whole picture is better understood in **Figs. 7** and **8**.

The realignment of spins is called spin echo. It is possible to apply many refocusing pulses after a 90° RF pulse, collecting many spin echoes as shown in **Fig. 8**. B_0 inhomogeneities are canceled in this method, because they are static in time, and

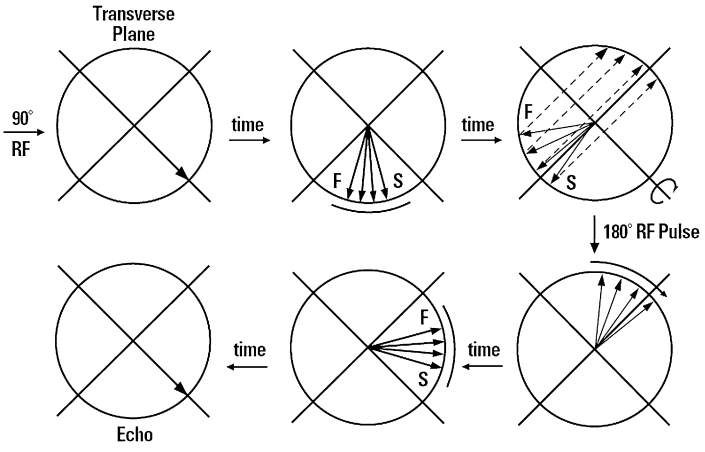

Fig. 7. The mechanism of spin echo with application of 180° RF pulse. (*Courtesy of* GE Healthcare, São Paulo, Brazil.)

the same B_0 inhomogeneity that spins feel before refocusing pulse they also experience after it. But spin-spin interactions are not static in time and T2 decay cannot be avoided. The longer the time a spin echo is collected, the stronger a T2 relaxation effect is presented.

Another important figure in pulse sequence is the repetition time TR, the time between 2 excitation pulses. In the spin echo sequence, TR is the time between 2 90° RF pulses applied in the same location.

TR and TE are the main parameters in spin echo sequence used to control contrast image weighting. Signal is acquired in echo time t = TE, and according to parameters set in the sequence, the spin echo received in the receiver coil will express differences among tissues, regarding proton density (PD), and T2 or T1 relaxation.

Consider 2 different magnetization vectors, M_a and M_b, possessing different PD, T1, and T2 properties. At equilibrium state, M vector magnitude depends on PD available in the tissue. A 90° RF pulse is applied in the system, and M_a and M_b relay into the transversal plane. Dephase between spins starts at different rates, and a refocusing pulse is applied at TE/2 to provide a spin echo at TE. If TE is short enough, T2 differences will not be relevant and the signal induced in the receiver coil will mostly represent PD properties. To fulfill this requisite, TR must be kept long enough, to allow M vectors to recover all their longitudinal magnetization and so that T1 differences will not influence M_{xy} vector after the next excitation pulse (**Fig. 9**). Therefore, PD-weighted images acquired with a spin echo sequence are obtained by using long TR and short TE.

If a T2-weighted image is desired, a long TR is needed to avoid T1 influence through excitation pulse repetitions, but TE must be adequate to reflect T2 relaxation differences in signal amplitudes acquired (**Fig. 10**). The optimal TE to optimize contrast between M_a and M_b is the time when the difference between transverse magnetization of M_a and M_b is larger. Therefore, T2-weighted images acquired with a spin echo sequence are obtained by using long TR and adequate TE.

To acquire T1-weighted images, a short TE is needed for a signal echo not to reflect T2 differences. After applying the first excitation pulse, M_a and M_b remain in a transversal plane and dephasing between spins is caused by T2*

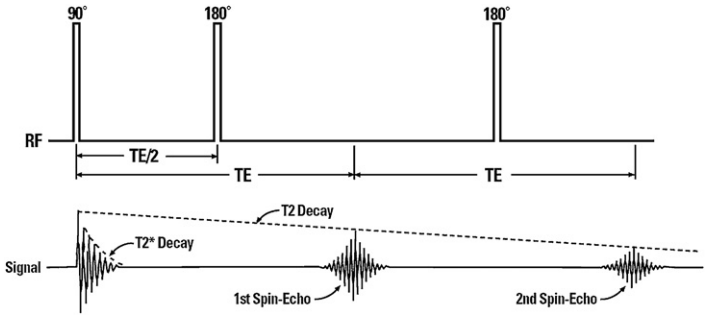

Fig. 8. A spin echo experiment with acquisition of 2 echoes. (*Courtesy of* GE Healthcare, São Paulo, Brazil.)

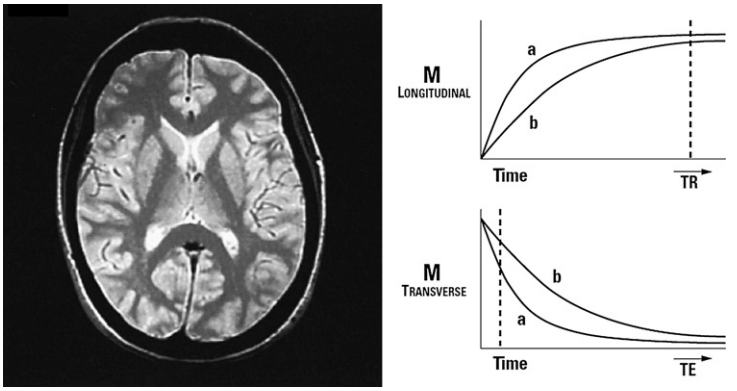

Fig. 9. Proton density–weighted image acquired using long TR and short TE. (*Courtesy of* GE Healthcare, São Paulo, Brazil.)

relaxation effects. The refocusing pulse is applied at a short TE/2 time and the first echo acquired represents PD differences. Then, T1 relaxation effects become significant and M_z recovery starts to M_a and M_b. In order that all the following echoes represent T1 differences, TR must be adequate and optimize T1 image contrast between M_a and M_b, and the next excitation pulse must be applied at the time when longitudinal magnetization M_a and M_b is larger (**Fig. 11**). Therefore, T1-weighted images acquired with spin echo sequences are obtained by using adequate TR and short TE.

Gradient echo (GRE) is another important pulse sequence that, instead of using RF pulses to refocus spins, uses a gradient pulse, referring to a controlled linear change of magnetic field strength during a short period. The gradient is characterized by its amplitude, representing how much field strength has changed in a certain distance, and its polarity, representing the direction of the change in field strength.

In a GRE experiment, an excitation and 2 gradient pulses are applied with different polarities and duration. The first gradient pulse is applied after the excitation pulse. While the first gradient is turned on the magnetic field amplitude changes regarding spatial location, and spins precess at different frequencies according to the Larmor equation, causing a certain phase accumulation between them, and the signal diminishes. The first gradient is then turned off and the second gradient is turned on, with the same amplitude and different polarity. Spins forced to precess slower than that feeling B_0, in the presence of the first gradient, now are forced to precess faster in the presence of the second gradient and, after some time, the accumulated phase between spins is compensated by inducing a signal echo generated by a gradient: a "gradient echo."

B_0 inhomogeneities are not canceled in this method, because a gradient echo is acquired by manipulating the magnetic field, and the magnetic field felt by spins at the application of the first

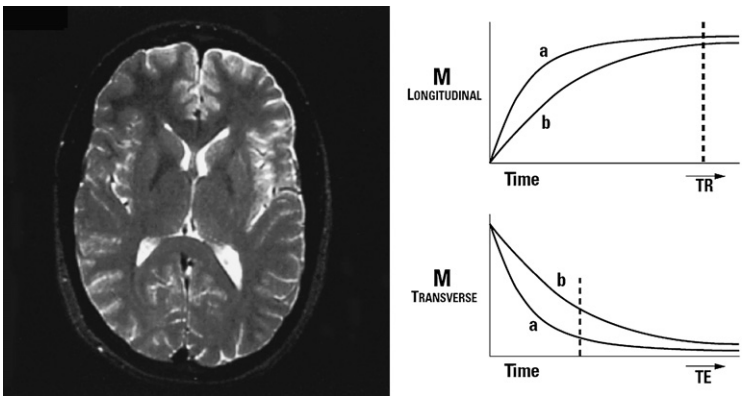

Fig. 10. T2-weighted image acquired using long TR and adequate TE. (*Courtesy of* GE Healthcare, São Paulo, Brazil.)

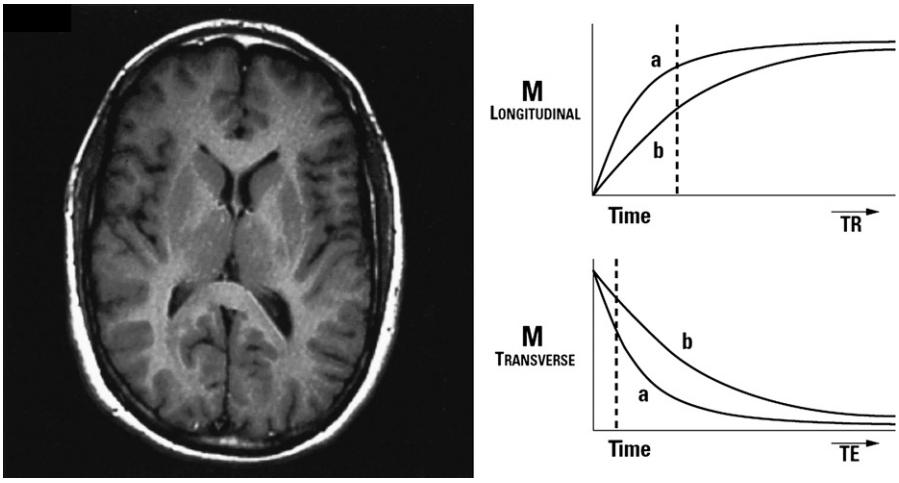

Fig. 11. T1-weighted image acquired using adequate TR and short TE. (*Courtesy of* GE Healthcare, São Paulo, Brazil.)

gradient is not the same in the presence of the second gradient.

Frequency and Phase Encoding

Pulse sequences are not used just to obtain different image contrasts but also to manipulate the spins and form an image. This manipulation is performed by turning gradients on and off, inducing phase and frequency for the spins, and using these properties as spatial information. GRE pulse sequence is used in the following explanation of image formation.

In a GRE pulse sequence, after the emission of excitation pulse, a gradient called "readout gradient" is applied, firstly with a negative polarity (to sample high frequencies of symmetric signal) and afterwards with a positive polarity to place spins in phase and read the echo. When this readout gradient, also known as frequency encoding gradient, is applied, H^+ spins precess at different frequencies at the same time the axis gradient was applied (**Fig. 12**).

Although the signal induced in the receiver coil contains all frequencies emitted by the tissues, there is a mathematical tool called Fourier transform (**Fig. 13**) that decomposes this signal in phases and frequencies. With the frequencies contained in the signal and the previous knowledge of the readout gradient amplitude applied, it is possible to correlate signal frequency and spatial location toward an applied gradient.

Unfortunately, it is not possible to apply the same strategy in the other axis, because it would change the spins frequency twice and only the last result would be obtained. To apply another gradient in other direction simultaneously would not be a solution, because magnetic fields would

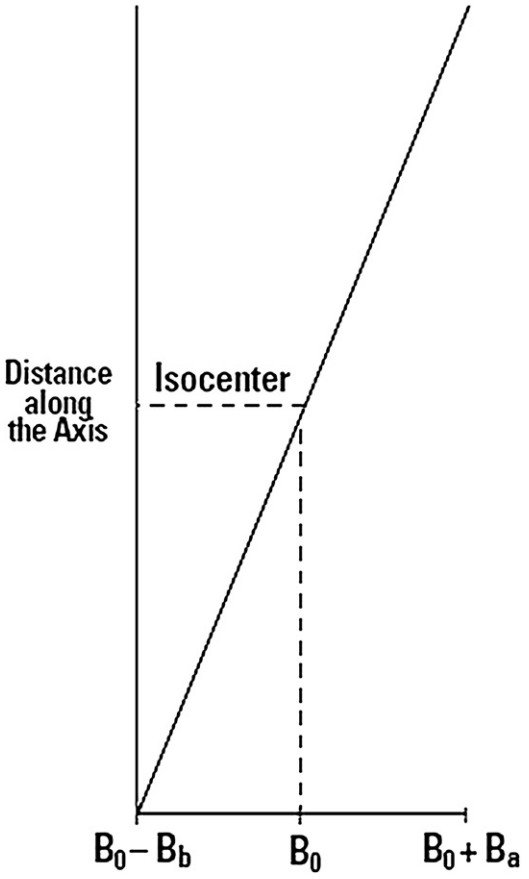

Fig. 12. During the application of a gradient, the magnetic field is modified linearly across the application direction. This change in magnetic field implies a change in precessional frequency, according to the Larmor equation. (*Courtesy of* GE Healthcare, São Paulo, Brazil.)

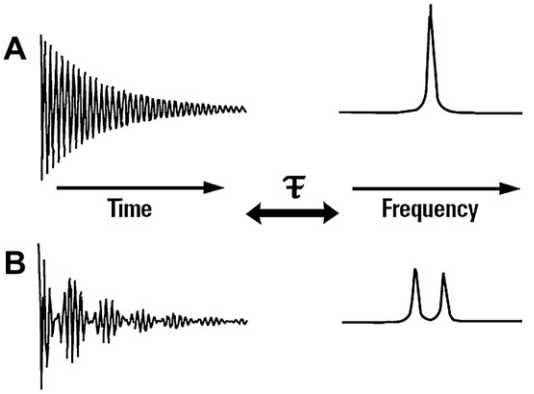

Fig. 13. The Fourier transform indicates the frequencies contained in the signal.

be vector summarized and just one frequency gradient would result. To solve this problem, phase information of spins is used. This information is added by applying a gradient called the "phase-encoding gradient" before the readout gradient and perpendicular to it. The phase-encoding gradient is kept for a short period to modify the magnetic field in the gradient direction, and during this short period spins precess at different frequencies according to equation (1). When the phase-encoding gradient is turned off, spins precess at the same frequency again, but they keep the phase memory acquired in the presence of the gradient (**Fig. 14**). The accumulated phase between spins depends on the gradient amplitude and duration.

In the sampling time, each part of the subject to be imaged will possess a bulk of spins with different phase and frequency information, making possible the image formation. The pulse sequence cycle must be repeated until K-space is filled in a proper way to form the final image.

K-Space and Acquisition Time

After frequency and phase encoding, a continuous signal emitted by the object to be studied is received by the receiver coil and sampled by the equipment, becoming a discrete signal. The signal sampled is converted in voltage and organized in the K-space, which holds the raw data of the image. As the signal is encoded in phase and frequency, both are the coordinates of K-space (**Fig. 15**). The inverse Fourier transform of K-space signal magnitude is the usual magnetic resonance image, thus a good coverage of K-space is needed to guarantee a reasonable image quality.

Pulse sequence controls K-space coverage. The phase-encoding gradient indicates the starting line in K-space to signal sampling, and the frequency-encoding gradient indicates the sampling direction on this line. Refocusing pulses to echo acquisition inverts the sampling direction.

The number of sampled points in K-space must be higher or equal to the number of pixels that compose the final image, thus pulse sequence must be repeated *n* times, varying the phase-encoding gradient amplitude to the entire coverage of K-space, where *n* corresponds to the matrix value in the phase direction; this is the first factor that hampers image acquisition time. The frequency encoding does not have a significant impact in acquisition time, because it takes the readout gradient duration (on the order of milliseconds). Nevertheless, the phase encoding to receive one echo depends on the application of one RF pulse, and TR must be taken into account for image contrast. Therefore, TR and phase-encoding steps are primarily the main aspects that affect image acquisition time, and usual methods that optimize acquisition time are multislice acquisition (excitation of multiple slices inside

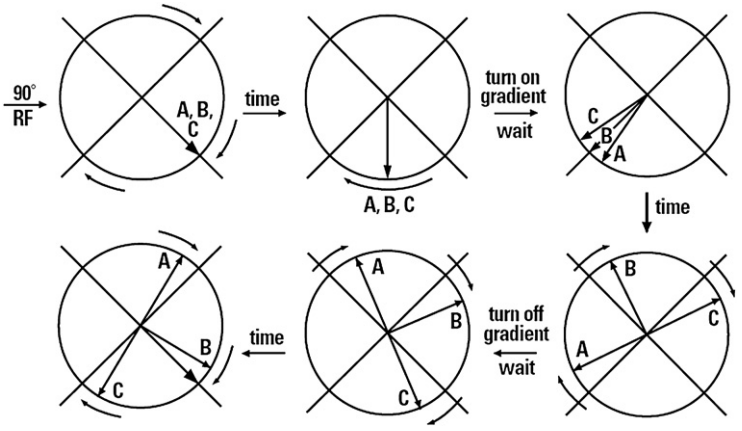

Fig. 14. Phase-encoding scheme representing 3 spins at different locations. (*Courtesy of* GE Healthcare, São Paulo, Brazil.)

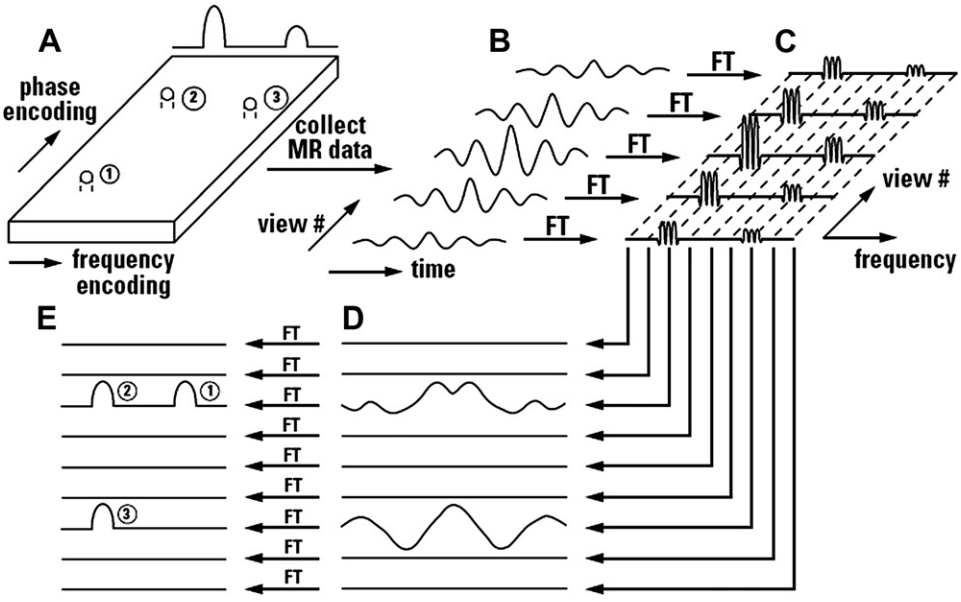

Fig. 15. Image formation by phase and frequency encoding using Fourier transform. (*A*) Slice representation with 3 vials of water. (*B*) Spin echo acquired from the entire slice with different phase encoding. (*C*) Fourier transformation of the signal. (*D*) A new data set is assembled from the columns in (*C*). (*E*) Inverse Fourier transform of (*D*) produces the image. (*Courtesy of* GE Healthcare, São Paulo, Brazil.)

a TR) and acquisition of multiple phase-encoding steps inside a TR, using either RF pulses or readout gradients, between phase-encoding steps.

INTRODUCTION TO DIFFUSION MR IMAGING

Principles and Concepts

Diffusion refers to the transport of gas or liquid molecules through thermal agitation randomly, that is, it is a function of temperature above 0 K. In pure water, collisions between molecules cause a random movement without a preferred direction, called Brownian motion. This movement can be modeled as a "random walk," and its measurement reflects the effective displacement of the molecules allowed to move in a determined period. The random walk is quantified by an Einstein equation: the variance of distance is proportional to $6Dt$, where t is time and D is the proportionality constant called the diffusion coefficient, expressed in SI units of m^2/s.

According to Fick's law, diffusion also occurs from a region of higher concentration to a lower concentration.

In biologic tissue, there is a high probability that water molecules interact with structures such as cell membranes, macromolecules that reduce or impede its motion (**Fig. 16**). Water exchange, between intracellular and extracellular compartments, as well as the shape of extracellular space and tissue cellularity, affects diffusion. In this case, the term apparent diffusion coefficient (ADC) represents the measured diffusion constants and is commonly reported in cm^2/s or mm^2/s.

Isotropy and anisotropy

Isotropy means uniformity in all directions. A drop of ink placed in the middle of a sphere filled with water spreads over the entire volume, with no directional preference. If the same experiment is repeated in a sphere filled with uniform gel the restriction is increased as compared with free water, but is still isotropic, as the restriction is the same in all directions.

Anisotropy implies that the property changes with the direction. If a bundle of wheat straw with the fibers parallel to each other is placed inside a glass of water, the ink will face severe restriction in the direction perpendicular to the fibers and facilitated along the fibers. This bundle is highly anisotropic (**Fig. 17**).

Diffusion-Weighted Imaging

MR image contrast is based on intrinsic tissue properties and the use of specific pulse sequences and parameter adjustments. The image contrast is based on a combination of tissue properties and is denominated "weighted," as the contribution of different tissue properties are present, but one of them is more expressive than the others.

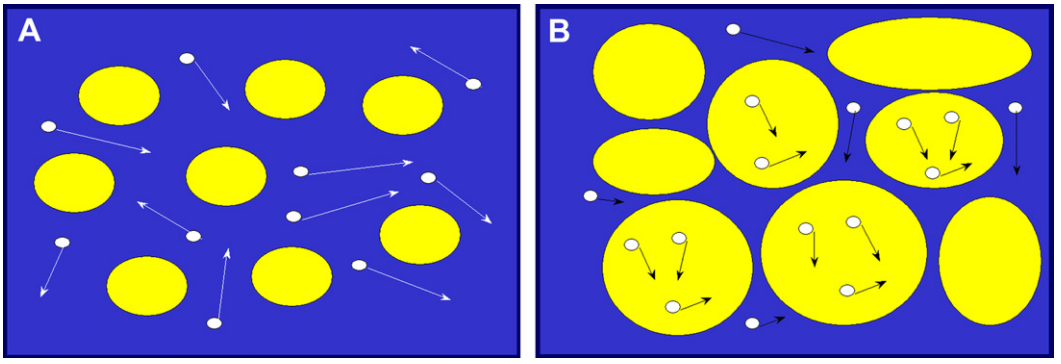

Fig. 16. (*A*) Water molecules travel by "random walk" more freely than (*B*), as the freedom of this movement is reduced by barriers as cell membranes. The diffusion in (*B*) is restricted as compared with (*A*). Finally, ADC (*B*) is less than ADC (*A*). (*Courtesy of* GE Healthcare, São Paulo, Brazil.)

Routine acquisitions have some degree of diffusion influence that is actually quite small. Some strategies have been developed to make diffusion the major contrast contributor, and dedicated diffusion-weighted imaging (DWI) sequences are available nowadays on commercial scanners, as well as several others as investigational sequences that may or not be available in clinical practice.

Diffusion sensitization scheme

Stejskal and Tanner[7] introduced a method to image and quantify DWI with MR imaging in 1960, which was implemented in routine practice by Le Bihan and colleagues[8] in 1986. The sequence was based on a spin echo sequence that has symmetric diffusion sensitizing gradients inserted before and after the 180° refocusing pulse (**Fig. 18**). The idea is as follows.

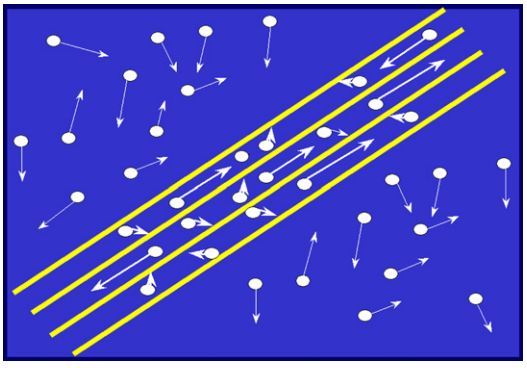

Fig. 17. The bundle offers no resistance to water molecules in the diffusion direction parallel to the fibers but there is a severe restriction if perpendicular. In this case there is preferred water molecule direction due to anisotropy. Outside the bundle, the water molecules are in an isotropic environment and have no preferred direction. (*Courtesy of* GE Healthcare, São Paulo, Brazil.)

Static water spins will experience a precise dephase induced by the first diffusion sensitizing gradient lobe. The 180° pulse will cause a phase compensation for the external field inhomogeneities. The second lobe will rephase the water spins at the same amount they were dephased, as the area is exactly the same and spins were in the same position. Therefore, the signal of the stationary water spins echo is maintained as practically unaltered.

However, moving water spins will be in a different position, so they will not be rephased at the same amount by the second lobe, and the echo will have a reduced signal. The degree of water motion is proportional to the signal attenuation.

The diffusion-sensitizing gradients can be applied to x, y, or z axes, as well as in a combination of them. This direction is called the diffusion-sensitizing direction.

The Stejskal-Tanner scheme can be applied on top of pulse sequences as spin echo, but the most used nowadays is in combination with spin-echo

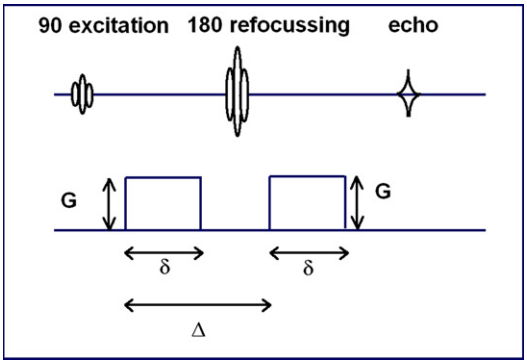

Fig. 18. Stejskal-Tanner Scheme: 2 diffusion-sensitizing gradients inserted before and after 180° RF refocusing pulse using precisely controlled duration and distance. G, amplitude; δ, duration of the sensitizing gradient; Δ, time between the 2 sensitizing gradient lobes.

echo-planar imaging (SE-EPI). A combination with fast spin echo sequence takes longer, but is less sensitive to distortions and susceptibility artifacts than EPI.

Other strategies are also available but are less used in routine practice, as many others are in the research environment and become commercialized eventually.

Diffusion-weighting factor

The sensitivity of the diffusion sequence to water motion can be varied by changing the gradient amplitude, the duration of the sensitizing gradients, and the time between the gradient pair.

The diffusion-weighting factor is named b-value and for the Stejskal and Tanner[8] sequence the value is given in units of s/mm^2 by (2):

$$b = \gamma^2.G^2.\delta^2(\Delta - \delta/3) \quad \textbf{(2)}$$

where γ is the gyromagnetic ratio, G is the strength of the diffusion-sensitizing gradients; δ is the duration of the gradient pulse, and Δ is the time interval between these gradients. A higher b-value is achieved by increasing the gradient amplitude and duration and by widening the interval between the gradient lobes. In most applications, the gradient amplitude is maximized and the gradient duration and interval changed to control the b-value.

The T2 shine-through phenomena

The signal intensity observed in a diffusion-weighted image can be expressed as:

$$S_{(TE,b)} = PD\left(e^{-TE/T2}\right)\left(e^{-bD}\right) \quad \textbf{(3)}$$

where S is signal intensity, k is a constant; PD is proton density, TE echo time, D diffusion coefficient, and b the b-value.

As TR (repetition time) is usually long (5000−15,000 ms) and, in case of single shot scans, TR is virtually infinite, T1 contamination is minimal or null. TE is usually kept as low as possible, usually 60 to 100 ms; therefore, the DWI may suffer from T2 contamination if long T2 components are present. This phenomenon is called the "T2 shine-through artifact" and may cause misinterpretation as the signal may be artificially hyperintense or isointense. Parametric ADC maps are used to quantify diffusion, and are insensitive to T2 shine-through artifacts.

Intravoxel incoherent motion

Intravoxel incoherent motion (IVIM) is the random movement of the water inside a voxel, and causes the signal to decay. One example is blood inside tortuous capillary vessels, where the measured diffusion coefficient will be overestimated and fall into the ADC denomination, instead of D. In 1988 Le Bihan and colleagues[9] proposed the name IVIM, instead of diffusion imaging, and D^* as the pseudo-diffusion coefficient dependent on capillary geometry and blood velocity, estimated to be 10 times larger than the diffusion coefficient of water. For high b-values, the perfusion effects are significantly reduced and diffusion information remains. For low b-values, the combined effect of perfusion and diffusion is present. As IVIM measurement involves the acquisition of several small b-values,[10] eddy currents must be well compensated, and motion and single-shot EPI diffusion must be used with high-performance gradients.

Echo-Planar Diffusion-Weighted Sequence

Echo-planar is an ultrafast acquisition, in which all K-space is sampled extremely fast. Although proposed by Peter Mansfield in 1978,[11] it was implemented in routine practice in the 1990s, when high-performance gradients and enhanced analog-to-digital converters, image reconstructors, and support electronics became available. It is fast, robust, and widely available on most scanners today, but it is also sensitive to susceptibility effects that cause artifact and image distortions. The distortion degree depends on several imaging parameters, as well as magnetic susceptibility and field strength.

EPI principles

The EPI strategy to reduce acquisition time is to collect several echoes, with phase and frequency encoding, after the RF excitation pulse, the same way as fast spin echo, but instead of producing an echo train using RF 180° refocusing pulses, EPI uses a series of oscillation gradient reversals that have both positive and negative polarities, to generate "odd" and "even" echoes that take significantly less time to be generated (**Fig. 19**).

EPI can be implemented using different modes such as SE-EPI (spin-echo EPI) or GRE-EPI (gradient-echo EPI), depending on the use of an RF echo or a gradient echo before the EPI echo train. It can collect all echoes needed to acquire an image by using one excitation pulse (single-shot EPI), or splitting into separate shots. SE-EPI is used in conjunction with diffusion-sensitizing gradients, called EPI-DWI, and the single-shot approach is mostly used.

EPI sequences are sensitive to the so-called off-resonance effects of water and fat spins: fat spins accumulate a huge phase shift, proportional to time, in collecting all echoes in a given TR and the frequency distance between water and fat. The effect occurs in the phase direction, and the image of fat can be typically displaced by pixels and is

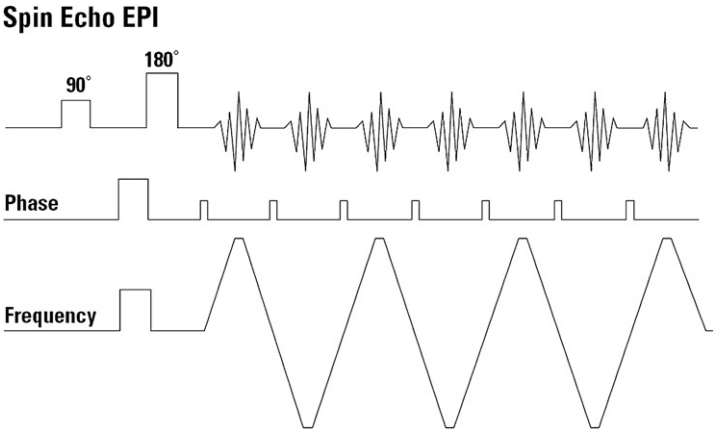

Fig. 19. After a 90° excitation pulse and 180° refocusing pulse is applied, positive-negative gradient oscillations generate frequency-encoded echoes, and the phase encoding is provided by the "blipped" phase encoding gradients. In this case there is an echo train length of 7. (*Courtesy of* GE Healthcare, São Paulo, Brazil.)

increased at higher field strengths. Therefore all EPI sequences, in practice, are fat-suppressed, and different methods can be employed such as spatial-spectral fat suppression, frequency-selective fat suppression, or even short-tau inversion recovery (STIR) in combination with EPI-SE.

The sampling period is typically the "flat-top" part of the readout gradient (**Fig. 20**A). Water spins also accumulate phase shifts in areas near tissue-air or tissue-bone interfaces, which cause disruptions in the local field, and the results are mild to severe distortions depending on the field strength, gradient performance, and sequence parameters (compare **Fig. 20**B with C). The longer the sampling time to collect the echo, the more time water spins accumulate phase shift and the worse is the distortion. The echo spacing is the time from the middle of the echo top to the middle of the next, and is directly related to the degree of the distortions. The shorter the echo spacing, the less the distortions; this concept is important to optimize sequence parameters and achieve the best results.

High-performance gradients using appropriate acquisition parameters improve EPI image quality significantly (see **Fig. 20**C).

EPI-DWI practical aspects

A common implementation of EPI-DWI acquires 3 separate orthogonal acquisitions with diffusion sensitization in each main gradient direction (X, Y, Z), which are automatically averaged into a final combined image (**Fig. 21**). Usually, 2 b-values are acquired, the first of which is generally b = 0 and is called "T2 image," as no diffusion contribution is present and it is the same as a T2-weighted EPI image. Different implementations allow the acquisition from a single to several b-values in the same scan, at the expense of acquisition time. Respiratory and cardiac compensation can be used to

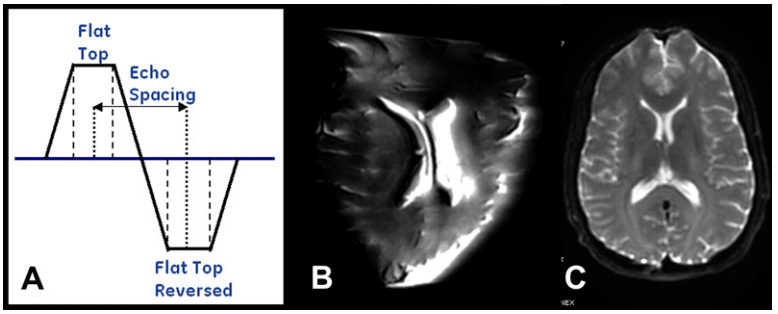

Fig. 20. (*A*) Detail of the oscillating readout gradient echo spacing. Reduction of echo spacing greatly reduces distortion. (*B*) Single-shot EPI with 256 frequency matrix, resulting in severe distortion in the phase-encoding direction on a low-performance gradient of 10 mT/m with 17 T/m/s slew rate. (*C*) Single-shot EPI with 256 frequency matrix, with a gradient of 33 mT/m with 120 T/m/s slew rate. (*Courtesy of* GE Healthcare, São Paulo, Brazil.)

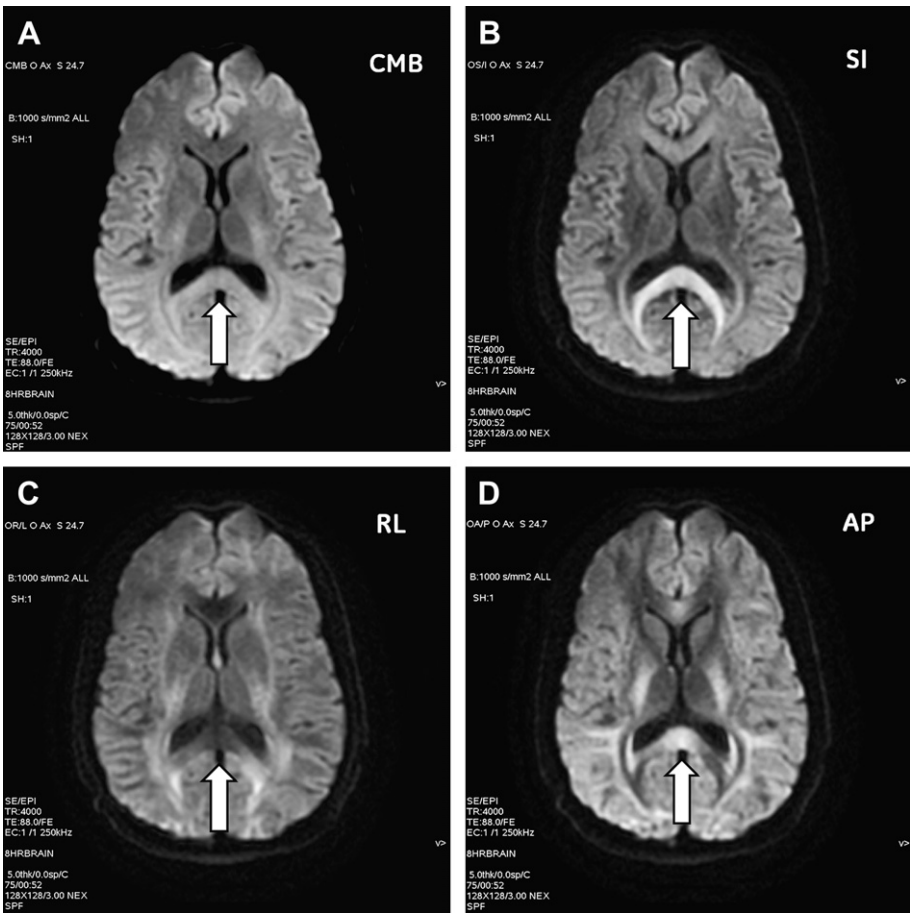

Fig. 21. The diffusion sensitization gradients were applied in directions SI (*B*), RL (*C*), and AP (*D*). Image (*A*) is the average of (*B*), (*C*), (*D*), and is usually denominated combined or "isotropic" image. The white arrow points to splenium of corpus callosum that has restricted diffusion in the SI direction, is facilitated in the RL direction, and has mixed pattern in the AP direction. Combined image (*A*) minimizes the anisotropy effects of the individual images.

minimize motion artifacts, as well as parallel imaging and optimized application of diffusion gradient schemes to improve signal-to-noise ratio and reduce artifacts.

The main sequence parameters are summarized as follows.

Choice of sensitizing directions and combined image The number of sensitizing directions and orientation used depends on the kind of information needed and the isotropic/anisotropic behavior of the structure being studied.

If the goal is to identify areas of altered diffusion in a structure that is normally isotropic, and considering the altered area is also isotropic, one direction would be enough. In this case, the total acquisition time is reduced to a single acquisition per b-value.

A more complex scenario is presented if the object of study and/or the expected altered area of interest are anisotropic. It is important to remember that the diffusion sensitization gradient will affect spins moving along its direction only. Organs such as the brain, kidneys, and muscles have important anisotropy, as others have a more isotropic behavior. This scenario is exemplified in **Fig. 21**: the splenium of the corpus callosum shows restricted diffusion in the SI (superior-inferior) direction (see **Fig. 21**B) and is facilitated in the RL (right-left) direction (see **Fig. 21**C), because of the orientation of the fibers that induces strong directional diffusion dependence. Notice the low-bright pattern in the AP (anterior-posterior) as the inverted "V" disposition of the fibers. In this instance, acquiring diffusion imaging, sensitized in the 3 directions, and averaging them

into one combined image is the most used strategy (see **Fig. 21**A).

b-Value The b-value provides diffusion weighting for DWI images as TE provides T2 weighting for T2 images.

The higher the b-value, the more diffusion-weighted the image will be at the cost of signal-to-noise ratio (SNR). As b-value is increased, a structure of lower ADC loses signal faster than structures of higher ADC, and the contrast is increased. If the lower ADC regions have the signal decreased from a certain threshold, the combined image may exhibit increased signal from restricted water motion, due to anisotropy. An example is given in **Fig. 22**.

If the b-value is high enough, only structures with very low ADC will show up and higher ADC structures will fade into the noise floor; this approach can be used as "background suppression" and increase sensitivity. As the minimum TE is increased with the b-value, relatively short T2 tissues such as liver and muscle may be suppressed because of T2 effects rather than diffusion, and this should be taken in account regarding choice of diffusion sequence parameters.

Low b-values have intrinsically high SNR; however, IVIM effects become important and should be taken into consideration. An interesting property is that flow is suppressed, and "black-blood "imaging can be performed (**Fig. 23**).

Receiver bandwidth Receiver bandwidth (rBW) controls the number of frequencies that are detected. The higher the rBW, the shorter the "flat-top" or readout time, and the fewer the distortions present (**Fig. 24**). Therefore, higher rBW is preferable for EPI-DWI studies.

Frequency direction Echo-planar acquisitions are sensitive to water off-resonance spins in the areas of soft tissue/air/bone interface. With a proper choice of frequency direction, the distortion is more symmetric (**Fig. 25**). Axial plane is the most commonly used acquisition plane with EPI and frequency RL direction.

Fat suppression Due to the large chemical shift, all EPI-DWI acquisitions should be fat-suppressed or fat-saturated. The choice of the method to be employed depends more on the region to be studied. Spectral spatial excitation excites only the water spins on a slice-by-slice basis, instead of the whole volume. Chemical shift selective applies a spectral saturation pulse over the fat spins, but it may be less effective than spectral spatial excitation once the fat saturation pulse is applied over the entire volume. STIR is a good option for a large field of view (FOV), off-center acquisitions, or areas where the other techniques may fail, such as brachial plexus.[12]

Number of measurements The data are acquired several times and averaged into one image, then used to build more SNR, allowing the acquisition of thinner slices and longer b-values at the expense of acquisition time. If motion is present as free-breathing scans in abdomen and chest, some degree of blurring is expected, as the structures are not in the same position in each acquisition and are averaged out. Small structures and

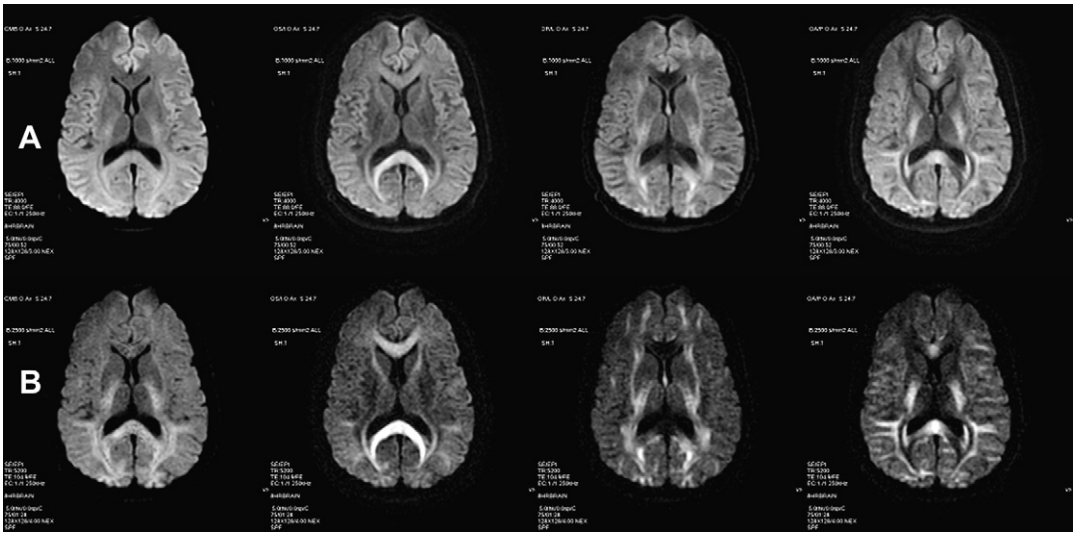

Fig. 22. From right to left the sensitization directions are: combined, SI, RL, and AP. Row (*A*) b = 1000 s/mm^2, TE = 88 ms; Row (*B*) b = 2500 s/mm^2, TE = 104 ms.

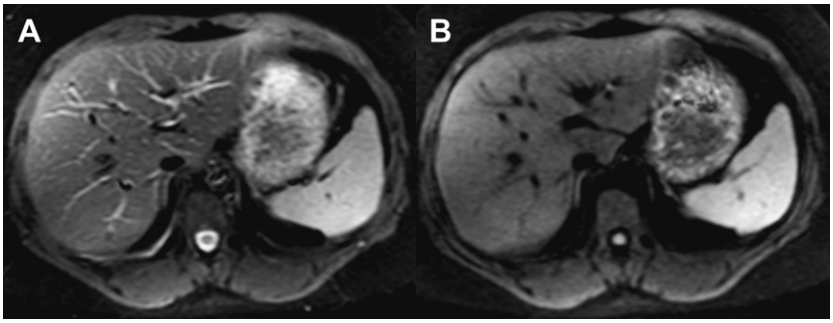

Fig. 23. Diffusion is inherently a black-blood image. Image (*A*) b = 0 s/mm^2, usually named "T2 image," and Image (*B*), usually named "diffusion image," have b = 90 s/mm^2.

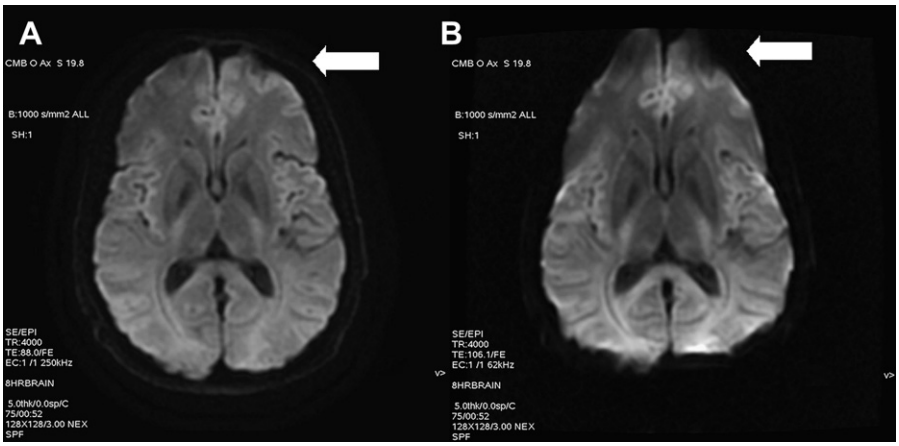

Fig. 24. (*A*) High rBW = ±250 kHz, (*B*) Low rBW = ±62 kHz; both at 3 T field strength. Distortion is reduced using high bandwidth. The unit of the receiver bandwidth can change between vendors, as peak to peak or Hz/pixel, and lead to mistakes if protocol parameters are copied without proper adjustment.

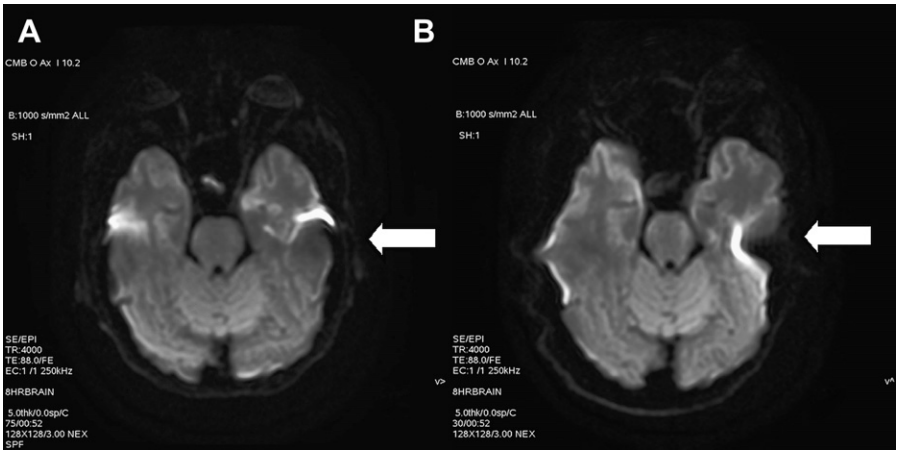

Fig. 25. Frequency direction (*A*) RL and (*B*) AP. (*A*) is more symmetric. Both images were acquired at 3 T field strength.

motion-ghosting artifacts may not show up in the final image as well, due to averaging.

The use of one single acquisition may require adjustment of other parameters, as increased slice thickness or lower acquisition matrix to compensate for the reduced SNR.

Repetition time The number of slices available and acquisition time are proportional to the TR. A TR of 3000 ms is enough to minimize T1 effects and can be as long as needed to accommodate all slices required in one acquisition, typically 5000 ms. Reduced TR acquisition with reduced number of slices can be used to shorten breath-hold time in expiration, but multiple acquisitions are necessary to cover the entire volume, and each group of slices may not be perfectly aligned.

Echo time The TE should be as short as possible and should increase with the b-value. Reduced frequency matrix and the use of parallel imaging decrease the echo spacing, and therefore the minimum TE.

In cases where multiple b-value acquisitions and ADC quantification are needed, it is suggested to use the TE corresponding to the highest used b-value and keep it constant in all other acquisitions of b-values.

Respiratory/cardiac trigger Respiratory trigger synchronizes the acquisition with the respiratory movement, by acquiring data in the expiration phase, reducing movement artifacts, and allowing the use of more measurements with less or no blurring, besides improving lesion detection as compared with breath-hold.[13] It is mostly used for imaging the chest and upper abdomen. Total acquisition time is increased, as only part of the respiration/cardiac cycle is used. The effective TR depends on the respiratory frequency and can be increased using more respiration cycles, to accommodate the number of slices. Cardiac motion is a known source of artifacts (**Fig. 26**) and can be minimized with cardiac triggering and appropriate trigger delay,[14] but again at the expense of time.

Parallel imaging Parallel imaging plays an important role in EPI-DWI, as the distortion and short T2 blurring are reduced at the expense of SNR. This feat is accomplished by omitting lines of the K-space and increasing the distance between them, just like reduced-phase FOV, but eliminating wrap-around artifacts that use special algorithms and need some K-space reference lines. As such this could be either a separate mask acquisition or a built one, and rely on different coil element sensitivity. Because susceptibility effects are enhanced at higher field strengths, parallel imaging is routinely used at 3 T, in combination with EPI sequences, and could be considered optional, but is recommended at 1.5 T. Other benefits of parallel imaging are increased number of slices for the same TR and reduction of acquisition time.

ADC measurement and ADC maps

The diffusion images have a T2 weighting contamination, and long T2 regions may present an artificial signal enhancement, such as the T2 shine-through artifact. This sign can be removed using exponential images (**Fig. 27**C) that are simply the diffusion image (see **Fig. 27**B) divided by b = 0 image (see **Fig. 27**A), or by using parametric images where the contrast reflects the calculated ADC (see **Fig. 27**D). Gray scale is normally used on ADC parametric images: dark representing low ADC values and bright representing high ADC values. Color scale can be used with low ADC in red and high ADC in blue as a mnemonic for free water, using different colors between the 2 extreme thresholds. However, there is no standard for the use of color scale, and it may be confusing if not properly explained.

In general, ADC (or *D* depending on the definition) is calculated using b = 0 and another *b* that

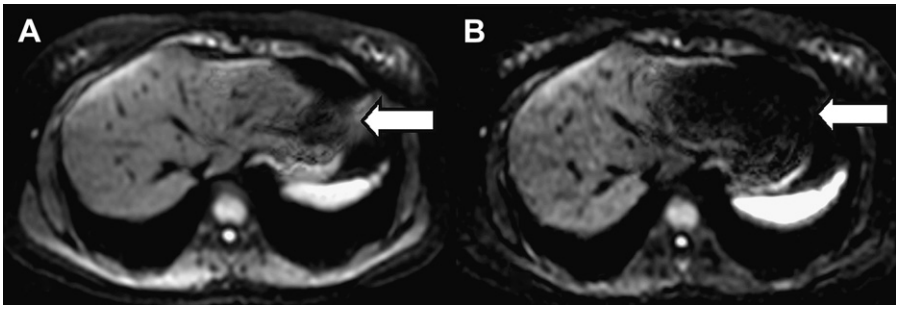

Fig. 26. Respiratory-triggered DWI, but not cardiac triggered. White arrows indicate cardiac motion artifact. (*A*) b = 150 s/mm^2 and TE = 54 ms; (*B*) b = 600 s/mm^2 and TE = 68 ms.

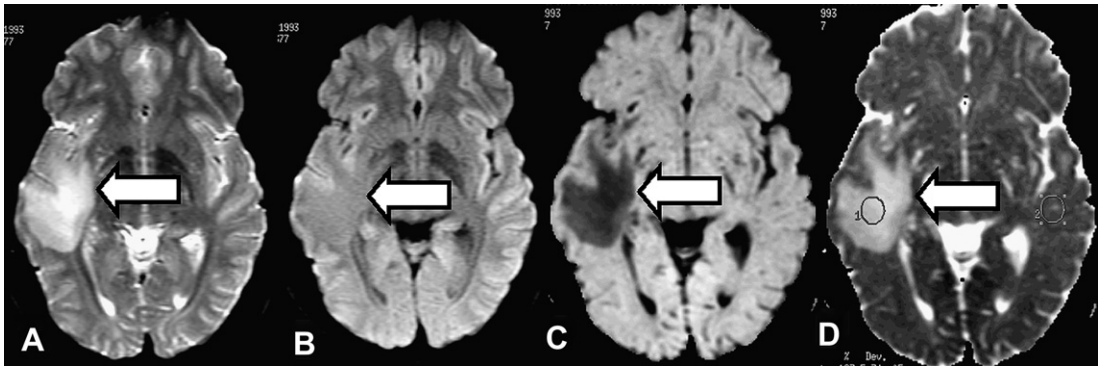

Fig. 27. Example of T2 shine-through effect and correction using exponential and parametric ADC maps: White arrow indicates bright signal on T2 image (*A*), isointense signal on diffusion image (*B*). The exponential map (*C*) has the T2 shine-through artifact removed and the expected low signal of facilitated diffusion is present. The parametric ADC map (*D*) demonstrates high ADC value as a bright region and enables quantification of ADC.

can vary, depending on the organ studied, usually between 600 s/mm^2 and 1000 s/mm^2.

Keeping the TR and TE the same and changing only the b-value, ADC can be calculated using the equation (4):

$$\mathrm{ADC} = \ln(S_1/S_0)/(b_1 - b_0) \quad \textbf{(4)}$$

where S_0 is the signal intensity with the b-value = 0 and S_1, the signal intensity with b-value = b. A monoexponential behavior is assumed.

In the context of research or clinical trial, a more precise estimation can be made using multiple b-values, and in this case, a more complex analysis is necessary because of the microcirculation influence.[9,10,15]

A plot of a multi b-value acquisition in a liver is exemplified in **Fig. 28**: respiratory trigger and b-values of 0 to 1000 s/mm^2. Notice the fast decay in the first part of the curve (b-values 0−100 s/mm^2), due to increased effects of microcirculation and a slower decay in the second part (b-values 200−1000 s/mm^2), due to increased effects of diffusion.

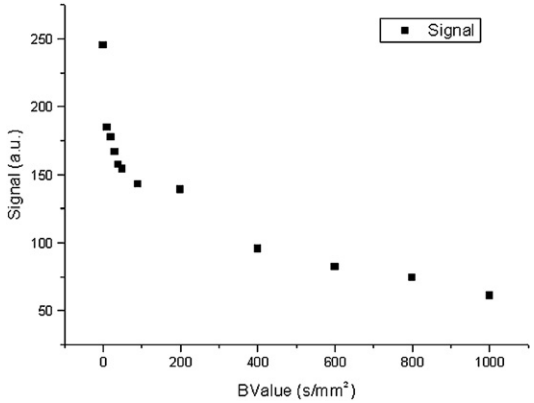

Fig. 28. Signal intensity versus b-value plot from a multi−b-value study on a liver. The signal decays faster between b = 0 and 100 s/mm^2.

The low range of b-values from 10 to 200 s/mm^2 may be used to study fast diffusion and is characterized by perfusion parameters D^* (or $\mathrm{ADC_{fast}}$) and f (fraction of volume of water flowing in capillaries). High b-values between 200 and 1000 s/mm^2, or higher, are used to study slow diffusion parameters D (or $\mathrm{ADC_{slow}}$). The term global diffusion is used when b = 0 and b > 200 s/mm^2, and is characterized as $\mathrm{ADC_{global}}$.

The quantification of ADC in moving organs or in the path of its influence is challenging, and the use of free breathing, respiratory triggering, or breath-hold may lead to different results and are under investigation.[16,17]

In summary, diffusion is used as a source of contrast for many different applications in the body, and gives insights on the pathologies by visual inspection. Also, there is a growing number of investigations using quantification; the total process is not completely understood, and a standardization of the acquisition and quantification is yet to be established.

Another aspect of diffusion, the anisotropy, is the study object of diffusion tensor imaging (DTI), which is now discussed.

DIFFUSION TENSOR IMAGING

DTI[18] is based on diffusion-weighted images that investigate the fiber architecture of several regions in the human body as for example of the brain white matter or muscle fibers of the heart. In contrast to DWI, a diffusion tensor $\underline{D}$ (a 3 × 3 matrix) is calculated for each voxel, instead of only one numerical value (such as the ADC), and it enables the possibility to investigate anisotropic

diffusion. Anisotropic diffusion means that the water molecules are moving in a specific direction at a specific rate, whereas isotropic diffusion means that the molecules move at equal rates in all directions. This tensor is able to fully describe the molecular mobility along each direction and the correlation between these directions.[18] To achieve this directional information, additional diffusion-weighted images along several gradient directions, using diffusion-sensitized MR imaging pulse sequences, have to be collected. After the postprocessing of the raw diffusion-weighted images, the fractional anisotropy (FA) maps, mean diffusivity (MD), eigenvectors, radial diffusivity, and so forth are calculated, derived from the diffusion tensor.

Physical Basics and Definitions

DWI and DTI use the mathematical model of free diffusion, which is described in physics by the "first Fick's law of diffusion." It can be written as:

$$J = -D\nabla c \quad (5)$$

where J is the flux density, ∇c the concentration gradient, and D the diffusion coefficient.

When diffusion occurs in the imaged volume, there will be attenuation, A, on the MR signal, which depends on D and on the "b-factor," which characterizes the gradient pulses used in the MR imaging sequence:

$$A = \exp(-bD) \quad (6)$$

In anisotropic media, the diffusion coefficient depends on the direction of diffusion. Leaving DWI and going to DTI, the diffusion coefficient D has to be substituted through a diffusion tensor $\underline{D}$ (a 3 × 3 matrix).

$$\underline{D} = \begin{pmatrix} D_{xx} & D_{xy} & D_{xz} \\ D_{yx} & D_{yy} & D_{yz} \\ D_{zx} & D_{zy} & D_{zz} \end{pmatrix} \quad (7)$$

To determine the diffusion tensor one must, as mentioned before, acquire diffusion-weighted images in several gradient directions. In a next step, it is necessary to estimate the entries of the matrix $\underline{D}$ from the set of diffusion-weighted images. As the tensor is symmetric, only 6 different gradient directions are necessary together with one acquisition with no diffusion weighting (b = 0) resulting in a total of 7 acquisition. Using more diffusion directions, it is not necessary, but of advantage, to cover the space more uniformly along many directions, especially for fiber orientation mapping.

Eigenvectors and eigenvalues, mean diffusivity, fractional anisotropy, radial diffusivity, and axial diffusivity

The entries of the tensor reflect average diffusion and degree of anisotropy in each voxel. It is important to determine the main directions of diffusivities, called eigenvectors, in each voxel, and the diffusion values, called eigenvalues, associated with these directions. The eigenvalues represent the diffusion coefficients in the main directions of diffusivities of the medium (Fig. 29). Most common parameters, such as MD, FA, radial diffusivity, and axial diffusivity can be derived from them.

The MD gives an overall measure of the diffusion in a voxel or region. It can be calculated from the trace of the diffusion tensor:

$$MD = Tr(\underline{D})/3 = (D_{xx} + D_{yy} + D_{zz})/3 \quad (8)$$

In the literature, the eigenvalues D_{xx}, D_{yy}, and D_{zz} are often called λ_1, λ_2, and λ_3.

The FA is a measure of the degree of the diffusion anisotropy. The FA values range from 1 (anisotropic diffusion = "directed") to 0 (isotropic diffusion = "not directed").

It can be calculated from:

$$FA = \frac{\sqrt{(D_{xx} - D_{yy})^2 + (D_{yy} - D_{zz})^2 + (D_{zz} - D_{xx})^2}}{\sqrt{2\left(D_{xx}^2 + D_{yy}^2 + D_{zz}^2\right)}} \quad (9)$$

The diffusivity along the main axis, D_{xx}, is also called axial diffusivity (or parallel diffusivity).

The average diffusivity $(D_{yy} + D_{zz})/2$ of the 2 minor axes is called radial diffusivity.

Visualization of the Tensor Model: the Ellipsoid Model

As the tensor data cannot be simply displayed in one image through gray-scale information or color coding, the diffusion ellipsoid approach has been presented.[19] The ellipsoid is a tridimensional representation of the diffusion distance in space, which the water molecules can reach. In the ellipsoid the x, y, and z axes represent the main diffusion direction in the voxel, corresponding to the direction of the fibers. The eccentricity of the ellipsoid provides information about the degree of anisotropy. This way, an anisotropic diffusion in any direction would be represented as a pole and an isotropic diffusion as a sphere (see Fig. 29).

Besides those representations, it is common to visualize FA and MD values in a gray scale or on a direction-coded color map (Fig. 30). Their values can be directly measured on these maps with

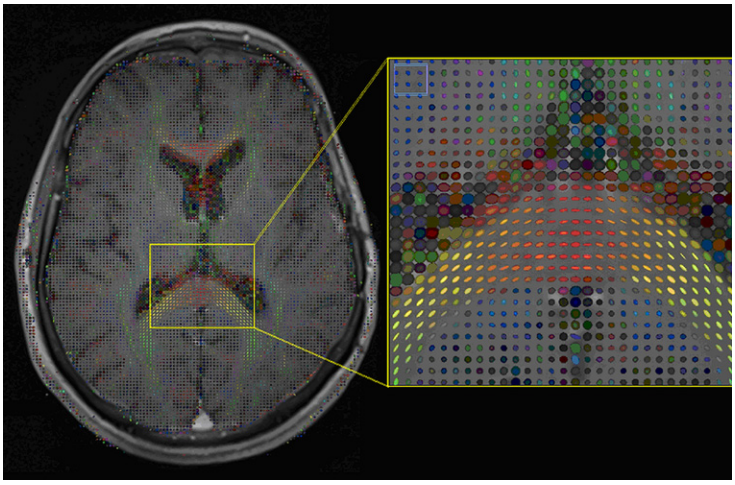

Fig. 29. (*Left*) The ellipsoid model overlaid on a conventional T1 image. (*Right*) The ellipsoid becomes a sphere in areas where no main diffusion directions exist: isotropic diffusion; and the ellipsoid becomes a pole with one main direction where the diffusion is anisotropic.

region of interest (ROI) tools provided by the software manufacturers.

Interpretation

In the brain, the mobility of the water molecules can be limited through obstacles, for example, the cellular membrane. Especially in the nerve fibers, the molecules can only move freely along the length of the axons and can only move short distances perpendicularly across the length. When interpreting diffusion tensor data, the basic idea is that the direction of the highest diffusion coefficient represents the course of the nerve fiber.

Tractography

The reconstruction of nerve fiber tracts of DTI data is called tractography. This technique is based on connecting voxels in order to build a whole fiber to investigate the fiber architecture in the brain. There are 2 major approaches in tractography: deterministic and probabilistic tractography. With deterministic tractography, the reconstructed fibers

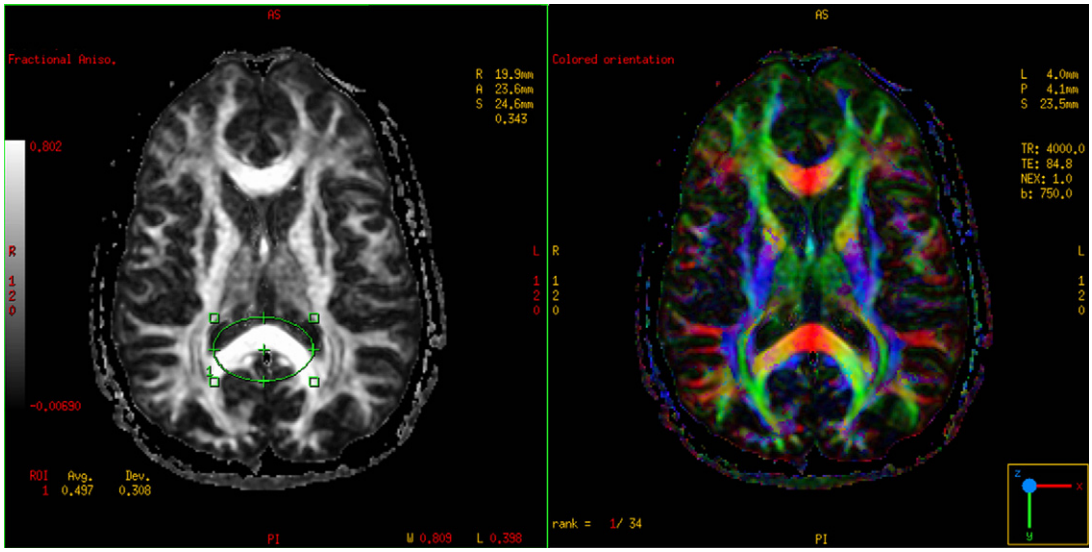

Fig. 30. (*Left*) Gray scale FA map, where the intensity value divided by 1000 corresponds to the FA value. Example: mean intensity value of the ROI of 831 corresponds to an FA of 0.831 in this ROI. (*Right*) FA map where the direction is color-coded.

result from the most likely directions in each voxel, whereas probabilistic fiber-tracking methods use probability distributions to draw several sets of different directions, this way repeating the streamlining process multiple times.

High Angular Resolution Diffusion Imaging

The diffusion-tensor model describes the behavior of diffusion in a voxel correctly only when the diffusion has one main direction. When nerve fibers cross with others or have ramifications, this model is limited. As a result, over the past few years approaches have been developed that aim to use more gradient directions, in order to gain a better insight into the complex behavior of diffusion. These techniques are called high angular resolution diffusion imaging or HARDI.

Number of diffusion directions

As mentioned before, at least 6 diffusion directions are necessary to determine the elements of the diffusion tensor. But what is the impact of using more directions and the relevance for clinical application? For a robust estimation (using a b-value of 1000 s/mm^2) of the FA, which was shown using a Monte Carlo technique, a minimum of 20 unique sampling directions should be used and 30 directions, at least, in the case of MD.[20]

Postprocessing and Evaluation of Diffusion-Weighted Images and Diffusion Tensor Imaging

Evaluation with manufacturers' software

Most MR manufacturers offer their own software to reconstruct the parametric maps for the diffusion parameters, such as ADC (in the case of DWI) and FA, MD, eigenvalues, and trace (in the case of DTI), that are most relevant for the radiologist. The reconstruction is normally performed in an in-line process, whereby the generations of those maps are performed automatically, immediately after running the sequence. In this way a rapid evaluation by the radiologist is possible.

Within the manufacturers' software, in general ROI-based analysis tools are available, enabling the radiologist to draw the ROI directly, such as for example the FA map, providing ROI parameters as the mean value, standard deviation, area, and minimum and maximum value. To obtain a "real" value for the diffusion parameters, sometimes a scaling factor has to be applied.

Region-of-interest based analysis is a common way to analyze, for example, differences in injured tissue with normal tissue (see **Fig. 30**).

Deterministic tractography (streamline tractography)

To reconstruct the trajectories of fibers, first at least one stream particle (seed point) has to be chosen (**Fig. 31**). Then the voxels are connected using pre-chosen calculation criteria for the tract, for example, angular threshold that determines the maximum orientation that a fiber can achieve and FA threshold that determines when the FA value falls below this threshold. Calculation for this tract can then be realized.

Advanced evaluation by third-party software

Instead of or in addition to the use of the software offered by the manufactures, or in addition to it, it is possible to realize advanced evaluation of the diffusion data with third-party software, after transferring the image volume to another workstation.

Especially for the brain, these software programs often offer additional tools that can be useful for analysis, as the image quality potentially can be improved. For instance, it is possible to apply eddy current correction algorithms in the EPI images, which take care of distortion artifacts. Also, distortions of the diffusion-weighted images caused by motion can be corrected. Especially for tractography, when one is interested in quantifying brain connectivity it may be interesting to use such software programs, because they can perform probabilistic tractography instead of more qualitative deterministic tractography offered by most MR manufacturers.

Another interesting option for institutions that are interested in clinical research is the possibility that comes with third-party software, namely the ability to carry out intersubject group analysis. The software includes tools for brain registration

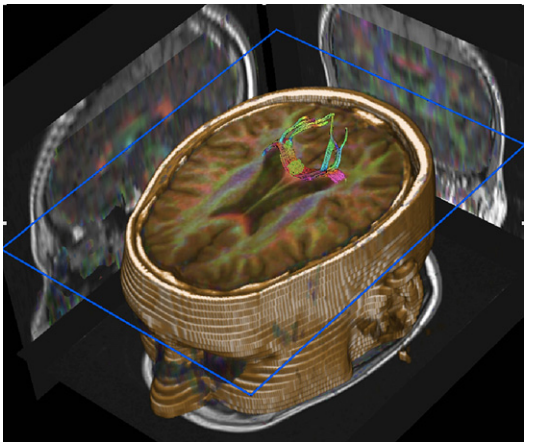

Fig. 31. After choosing a seed point the streaming of the fibers can be realized.

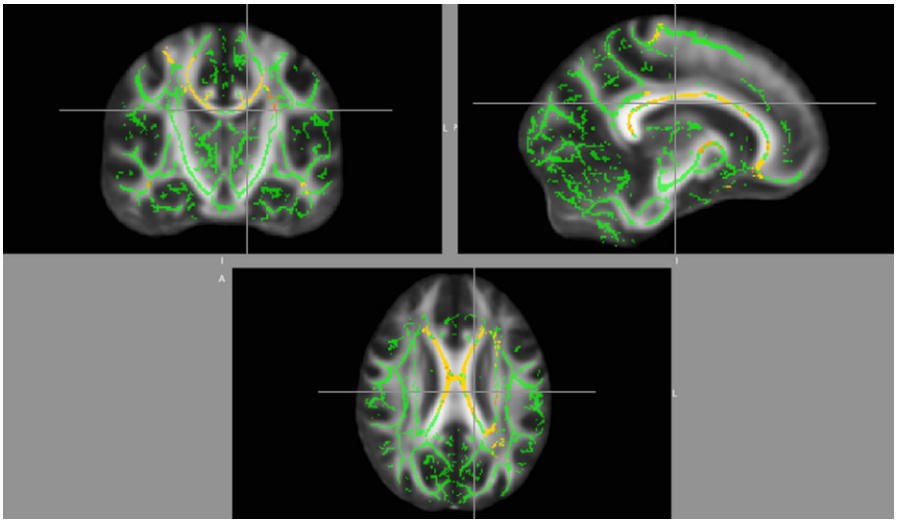

Fig. 32. Tract-based spatial statistical analysis (TBSS; FSL, Oxford, UK). In green: the main tracts (skeleton) where statistical analysis was performed. Overlaid in yellow-red: significant areas of reduction of FA, $P<.05$.

to a pre-chosen target, which may be a mean FA image of the subjects under analysis,[21] to perform voxel-based analysis of the whole brain, using brain atlases as a reference (**Fig. 32**).

REFERENCES

1. Haacke EM, Brown RW, Thompson MR, et al. Magnetic resonance imaging: physical principles and sequence design. Chichester (UK); New York: Wiley-Liss; 1999.
2. Damadian R. Tumor detection by nuclear magnetic resonance. Science 1971;171(976):1151–3.
3. Vlaardingerbroek MT. Magnetic resonance imaging: theory and practice. New York. 3rd edition. Berlin: Springer; 2003.
4. Lauterbur P. Image formation by induced local interactions: examples employing nuclear magnetic resonance. Nature 1973;242:190–1.
5. Mansfield P, Grannell PK. NMR 'diffraction' in solids? J Phys C Solid State Phys 1973;6(22):422–6.
6. Bitar R, Leung G, Perng R, et al. MR pulse sequences: what every radiologist wants to know but is afraid to ask. Radiographics 2006;26(2): 513–37.
7. Stejskal EO, Tanner JE. Spin diffusion measurements: spin echoes in the presence of a time-dependent field gradient. J Chem Phys 1965; 42(1):288–92.
8. Le Bihan D, Breton E, Lallemand D, et al. MR imaging of intravoxel incoherent motions: application to diffusion and perfusion in neurologic disorders. Radiology 1986;161(2):401–7.
9. Le Bihan D, Breton E, Lallemand D, et al. Separation of diffusion and perfusion in intravoxel incoherent motion MR imaging. Radiology 1988;168(2): 497–505.
10. Luciani A, Vignaud A, Cavet M, et al. Liver cirrhosis: intravoxel incoherent motion MR imaging—pilot study. Radiology 2008;249(3):891–9.
11. Mansfield P, Pykett IL. Biological and medical imaging by NMR. J Magn Reson 1978;29: 355–73.
12. Takahara T, Hendrikse J, Yamashita T, et al. Diffusion-weighted MR neurography of the brachial plexus: feasibility study. Radiology 2008;249(2): 653–60.
13. Taouli B, Sandberg A, Stemmer A, et al. Diffusion-weighted imaging of the liver: comparison of navigator triggered and breathhold acquisitions. J Magn Reson Imaging 2009;30(3):561–8.
14. Murtz P, Flacke S, Traber F, et al. Abdomen: diffusion-weighted MR imaging with pulse-triggered single-shot sequences. Radiology 2002; 224(1):258–64.
15. Thoeny HC, Ross BD. Predicting and monitoring cancer treatment response with diffusion-weighted MRI. J Magn Reson Imaging 2010; 32(1):2–16.
16. Nasu K, Kuroki Y, Fujii H, et al. Hepatic pseudo-anisotropy: a specific artifact in hepatic diffusion-weighted images obtained with respiratory triggering. MAGMA 2007;20(4):205–11.
17. Kwee TC, Takahara T, Koh DM, et al. Comparison and reproducibility of ADC measurements in breathhold, respiratory triggered, and free-breathing

diffusion-weighted MR imaging of the liver. J Magn Reson Imaging 2008;28(5):1141–8.
18. Le Bihan D, Mangin JF, Poupon C, et al. Diffusion tensor imaging: concepts and applications. J Magn Reson Imaging 2001;13(4):534–46.
19. Pierpaoli C, Basser PJ. Toward a quantitative assessment of diffusion anisotropy. Magn Reson Med 1996;36(6):893–906.
20. Jones DK. The effect of gradient sampling schemes on measures derived from diffusion tensor MRI: a Monte Carlo study. Magn Reson Med 2004;51(4): 807–15.
21. Smith SM, Jenkinson M, Johansen-Berg H, et al. Tract-based spatial statistics: voxelwise analysis of multi-subject diffusion data. Neuroimage 2006; 31(4):1487–505.